Available online at www.sciencedirect.com
ScienceDirect
Catalysis Today 133–135 (2008) 136–141
CATALYSIS TODAY
www.elsevier.com/locate/cattod

Characterization of ZnO and TiO_2 catalysts to hydrogen production using thermoprogrammed desorption of methanol

Deborah V. César, Rachel F. Robertson, Neuman S. Resende *

Programa de Engenharia Química/NUCAT, Universidade Federal do Rio de Janeiro/COPPE, Cidade Universitária, Centro de Tecnologia, Bloco G/115, CEP: 21945-970, Rio de Janeiro/RJ, Brazil

Available online 8 February 2008

Abstract

Mixed zinc, titanium and alumina oxides were characterized by X-ray diffraction (XRD) and TPD-methanol techniques. The surface properties were correlated with the products from methanol decomposition. XRD results showed that 20% of ZnO supported on Al_2O_3 and on TiO_2/Al_2O_3 formed zinc aluminate phase. However, 20%ZnO/TiO_2 and 20%TiO_2/Al_2O_3 presented the characteristic structure of the oxides as segregated phases. TPD-methanol results for 20%TiO_2/Al_2O_3 sample showed an intense CO desorption, which was associated with a large density of Lewis acid sites due to TiO_2 surface and to the Lewis and Brönsted acid sites of alumina. On the other samples, the higher density of basic sites and weak Lewis acid site was related to ZnO presence that increased the CO_2 desorption. The high H_2/CO_2 ratio and the absence of CO and other desorption products showed that ZnO/TiO_2 is a promising system to be used as support or catalyst to H_2 production employed in fuel cells.

Keywords: Zinc oxide; Titania; TPD; Methanol; Hydrogen production

1. Introduction

Fuel-cell powered vehicles using hydrogen are currently under extensive investigation. However, the use of hydrogen gas for vehicle applications is postponed by technical limitations associated with safety, storage and distribution [1]. Therefore, current trends indicate that vehicles equipped with fuel cells will use liquid fuels as hydrogen source, at least in the early stages of commercialization [2,3].

Methanol is potentially a good source of hydrogen, for the on-board production of hydrogen, due to its high hydrogen to carbon ratio, low boiling point and availability. The absence of carbon–carbon bonds in methanol drastically reduces the risk of coking. Methanol can also be produced from renewable resources and thus lowering the production of greenhouse gases [4].

The steam reforming of methanol has received much attention due to the ability to produce a gas with high hydrogen concentration while maintaining a high selectivity towards carbon dioxide. [3,5]. Fuels produced by steam reforming contain ≈70–80% hydrogen, those by partial oxidation ≈35–45%. Lower fractions of hydrogen in the fuel degrade fuel-cell performance. Steam reforming of methanol at moderate temperature (200–300 °C) mainly produces carbon dioxide and hydrogen, and only ~1–2%CO.

A proton exchange membrane (PEM) fuel cell can tolerate only minuscule quantities (10–20 ppm) of carbon monoxide in its feed. Brown [6] compares some advantages and disadvantages of various primary fuels suggested as hydrogen sources for PEM fuel cells. Methanol, natural gas, gasoline, diesel fuel, aviation jet fuel, ethanol, and hydrogen itself were evaluated in that work. He shows that all the other processes for creating hydrogen from organic-chemical fuels form large quantities of CO in their products, the amounts ranging from 10 to 25%.

Wasmus and Kuver [7] did a review about the development of the direct methanol fuel cell (DMFC), long being considered as the most difficult fuel-cell technology methanol crossover and catalytic inefficiency. In order to reduce the usage of precious metals they suggested that the best possible performance has to be extracted from a given amount of catalyst. This involves mainly catalyst preparation, pretreatment, electrode preparation and, in the case of supported catalysts, also the choice of a suitable support. Therefore, the

* Corresponding author.
E-mail address: neuman@peq.coppe.ufrj.br (N.S. Resende).

0920-5861/$ – see front matter
doi:10.1016/j.cattod.2007.12.089

development of methanol decomposition catalysts for on-board production of hydrogen is highly required.

Copper and zinc-based catalysts were often used because Cu/ZnO-based catalysts are industrial low-temperature methanol synthesis catalysts. However, it has been shown that these catalysts present rapid deactivation in the methanol decomposition environment [8]. On the other hand, a number of recent studies concerning the ZnO-based catalysts characterization under oxidizing conditions have revealed that the mechanisms, formation of surface species, as well as, oxide phases synergy remain attractive for investigation in the steam reforming process [3,9]. Studies carried through by Agrell et al. [10], about the reduction of CO in the product of the steam reforming of methanol, had used commercial $Cu/ZnO/Al_2O_3$ catalyst. It was observed that the addition of oxygen in the steam–methanol feed mixture, as well as, the reduction of the contact time and decreases temperatures, minimizes the CO production.

The acid-basic properties of the ZnO/Al_2O_3 system had been characterized in the literature [11,12] as a function of the zinc oxide content and of the temperature of calcination. It was shown that the aluminate phase formation, for contents above of 20%, and the increase of the calcination temperature, from 600 °C up to 800 °C, had caused significant changes in the acidity and the basicity of the sample. The methanol oxidation product distribution reflects the nature of the surface active sites since redox, acid, and basic sites yield formaldehyde (HCHO), dimethyl ether (CH_3OCH_3), or CO_2, respectively; however, most pure metal oxides produce CO*x* above 200 ± C due to the decomposition of surface formate species. [13,14].

Spectroscopic studies of adsorbed methanol and temperature programmed desorption (TPD) analysis has been used to characterize oxides surface showing that surface methoxy and formate species are generated upon exposure of metal oxides (Al_2O_3, ZrO_2, TiO_2, NiO, Fe_2O_3, ZnO, CuO, MoO_3, CeO_2, Co_3O_4) to methanol vapor [14]. In a previous study of our group [15] using FTIR and TPD, it was concluded that the addition of ZnO to Al_2O_3 is responsible for the reduction of the strength and the number of the Brönsted acid sites and that the nature of these acid sites depends on the phases present on the catalyst.

The goal of this work is to evaluate the effect of the surface properties of a series of ZnO and TiO_2 supported catalysts using methanol as a probe molecule on temperature programmed desorption analysis. The characterization of its active sites can be helpful in choosing the most suitable catalyst to be applied in the methanol combined reform reaction (partial oxidation + - steam reforming), aiming to H_2 production for fuel cells.

2. Experimental

2.1. Catalyst preparation

- γ-Al_2O_3: (Harshaw—Al3996), (200 mesh), calcined at 550 °C for 5 h, under airflow.
- TiO_2: it was prepared by slow hydrolyze of titanium isopropoxide ($Ti(OCH(CH_3)_2)_4$), dried at 120 °C for 19 h and calcined under air flow (60 ml/min) at 550 °C for 6 h.
- ZnO: it was obtained by slowly adding a 0.6 M Na_2CO_3 aqueous solution to a 0.6 M $Zn(NO_3)_2{\cdot}6H_2O$ aqueous solution. The precipitated was washed several times, dried at 100 °C and calcined under airflow at 500 °C for 6 h [12].
- 10% and 20%ZnO/Al_2O_3 (10ZnA, 20ZnA), 20%ZnO/TiO_2 (20ZnT) and 20%ZnO/20%TiO_2/Al_2O_3 (20ZnTiA): it was prepared by wetness-impregnation method, using $Zn(NO_3)_2{\cdot}6H_2O$. Calcination at 550 °C, 6 h under air flow.
- 20%TiO_2/Al_2O_3 (20TiA): it was obtained by wetness-impregnation technique, with ($Ti(OCH(CH_3)_2)_4$) under inert ambient. Calcination was carried out at 550 °C, 6 h under airflow. [16].

2.2. Catalyst characterization

- Superface area (BET method): it was determined by nitrogen adsorption at 77 K in Micromeritics equipment, ASAP 2000 model. The samples were pretreated under vacuum during the night at 300 °C.
- X-ray fluorescence (XRF): the testes were carried out in Rigaku instrument, RIX-3100 model, using Rh source, 50 KV and 80 mA.
- X-ray diffraction (XRD): the patterns were obtained with a Rigaku instrument Miniflex TG model, using Cu Kα radiation (30 KV e 15 mA). The step-scans taken over the range of 2θ from 10° to 90° in step of 0.05, the intensity data for each step was collected for 1 s. It was used ICDD-PDF-2 data for phase identification, by Hanawalt method.

2.3. Methanol temperature-programmed desorption (TPD-MeOH)

It was used a multipurpose unit equipped with an on-line quadrupole detector QUADSTAR 422 (QMS 200, Balzers). Initially the samples (100 mg) have been treated at 450 °C, under He flow (60 ml/min) for 1 h, at 10 °C/min and cooled down to room temperature (25 °C). At this temperature, He flow (60 ml/min) was switched and sent to Pyrex glass saturator that containing methanol at 25 °C. Then, the methanol vapor carried was introduced into the reactor for 30 min ensuring a saturated adsorption of methanol on the surface of catalysts. Afterwards, the catalyst was flushed with He (60 ml/min) for 30 min. TPD measurements were performed from room temperature to 800 °C at a heating rate of 10 °C/min with He as carrier gas. The desorbing species were monitored using the mass spectrometer. Multiple *m*/*e* ratios were collected during each TPD run. The ion/mass (*m*/*e*) signals with relative intensity monitored during the desorption had been: H_2: 2 (100%); He: 4 (100%); methane: 16 (100%), 15 (85.8%), 14 (15.6%); H_2O: 18 (100%); 17 (23%); 16 (1.6%); CO: 28 (100%), 12 (4.5%); N_2: 28 (100%), 14 (7.2%); methanol: 32 (66.7%), 31 (100%), 29 (69.4%); formaldehyde: 29 (100%), 30 (55%); CO_2: 44 (100%), 28 (11%), 16 (8.5%); dimethyl ether, DME: 45 (100%), 46 (61%), 29 (39%); methyl formate: 60 (38%), 31 (100%); dimethoxymethane, DMM: 75 (43.6%), 45 (100%), 29 (44%). Individual products were identified by their characteristic mass fragmentation patterns. The desorption

Table 1
Textural properties of binary and pure oxides

Sample	FRX	S_{BET}		V_p[a] (cm^3/g)	d_p[b] (Å)
	Oxide content (%)	(m^2/g)	(m^2/γ-Al_2O_3)		
Al_2O_3	100	183	–	0.57	121
TiO_2	100	59	–	0.18	124
ZnO	99.8	15	–	0.05	131
20ZnA	20.6	88	111	0.35	162
20TiA	22.8	128	166	0.37	116
20ZnTiA	21.6	112	185	–	–
20ZnT	21.5	7	–	0.07	292

[a] Pore volume.
[b] Pore average diameter.

spectra for specific molecules presented below have been corrected for overlapping cracking fragments from other products and quantified using standard procedures.

3. Results and discussion

The oxide loading and textural properties of the samples are shown in Table 1. It was observed a decrease in the specific surface area and in the pore volume (V_p) for the supported oxides when compared with the pure oxides. The deposition of TiO_2 (20TiA and 20ZnTiA) did not cause significant changes in the alumina textural properties, as observed for specific surface values normalized by Al_2O_3 weight (m^2/g alumina). For 20ZnT sample, it was observed a great decrease (~89%) in the specific surface area and an increase of the average pore diameter when compared with the pure titanium oxide.

XRD patterns of the pure oxides and catalysts are shown in Fig. 1. According to ICDD-PDF-2 reference data, it was observed that TiO_2 is formed mainly by anatase phase and alumina with gamma structure. XRD data obtained for supported oxides demonstrated that 20ZnA shows characteristics diffraction peaks of aluminate phase ($ZnAl_2O_4$) ($2\theta \sim 31.75^\circ$, 37.35°, 60° and 66.6°), which was formed by the migration of Zn^{2+} into alumina lattice [12]. In a previous study [15], we have verified that the aluminate formation is favored by the increase in the zinc oxide loading (from 8%). For 20ZnT, the zinc oxide as zincite and TiO_2 as anatase are present as segregated phases. This sample presented large and low intensity characteristics peaks, although the high ZnO loading (21.5%). It should be attributed to a low crystallinity. Higher size of the crystallites may be an indication of coalescence. Thus, it is possible that the observed changes in textural properties after zinc oxide impregnation (Table 1) could be due to that effect. Also, 20TiA sample presented low intensity peaks, although with high TiO_2 loading (22.8%) and were identified characteristics diffraction patterns of Al_2O_3 ($2\theta \sim 37^\circ$, 46° and 66.8°) and TiO_2 ($2\theta \sim 25$, 35°, 48°, 54° e 55°). It is an indicative of high dispersion and low crystallinity of the anatase phase, which is due to the preparation method used in this work [16]. The 20ZnTiA sample shows characteristics peaks related to gamma-alumina (γ-Al_2O_3) and anatase phase (TiO_2), while the zinc oxide phase presents diffraction peaks at $2\theta \sim 31.9^\circ$, 34.45°, 36.3° and 56.65°. It is worth noting that occurred an increase in the diffraction peaks intensity related to titanium oxide at $2\theta \sim 25.35^\circ$ and at $2\theta \sim 62.9^\circ$ related to both oxides, ZnO and TiO_2, respectively. Besides, new peaks at $2\theta \sim 60^\circ$ and 66.6° due to zinc aluminate with a spinel like structure were observed, which suggests changes in the crystalline structure and/or in the dispersion of the both ZnO and TiO_2 oxides. These changes allowed a higher interaction between the Zn^{2+} cations and alumina. This is in consistence with specific surface area normalized result (Table 1) for 20ZnTiA sample that was similar to the value for gamma-alumina.

Methanol TPD profiles for the zinc oxide catalyst supported on Al_2O_3 (20ZnA) are shown in Fig. 2 that consists of two regions of desorption, one between 60 and 300 °C and the second between 300 and 610 °C. It is interesting to observe the ion mass $m/e = 29$ that presented peaks at 120 and 230 °C. The first one is attributed to the molecularly adsorbed methanol ($m/e = 31$, not shown), as commonly observed after low adsorption

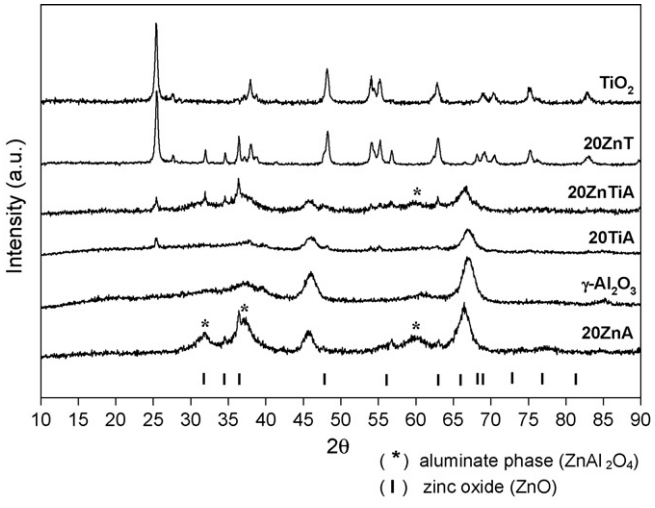

Fig. 1. XRD patterns of binary and pure titanium and zinc oxides.

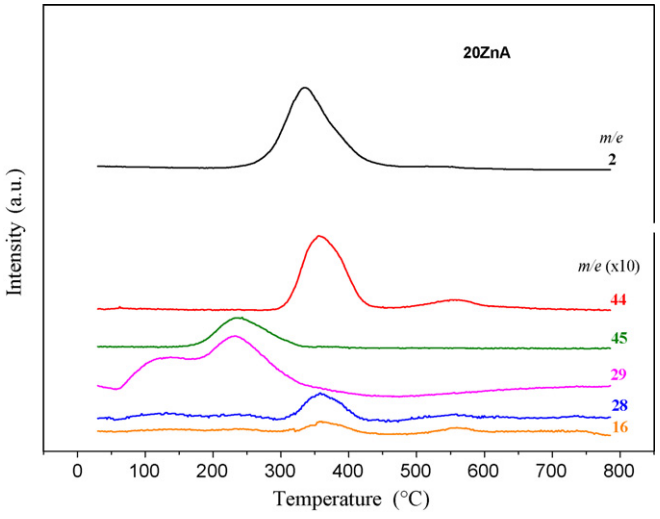

Fig. 2. TPD-MeOH profiles of 20ZnA catalyst.

temperature [17,18] and also to the formaldehyde desorption, as a product of the dehydrogenation reaction [19]. The peak at 230 °C is related to DME fragmentation (see *m/e* = 45), together with the water (*m/e* = 18, not shown), due to the dehydration reaction of the intermediate groups adsorbed on the surface. The literature [19–21] reports that primary alcohols adsorbs on the metallic oxide surfaces as alkoxide, from the scission of the OH bond. In general, the alkoxide species leave the surface by two ways: reacting with the surface hydroxyl, around 120 °C, and by decomposition at high temperatures [20]. According to Yee et al. [21], on some oxide surfaces dehydrogenation reaction occurs to form aldehydes from primary alcohols. On the basis of this, the 20ZnA TPD profiles suggest that methanol forms methoxy groups as intermediates (–O–CH3) and yields DME and formaldehyde, which can quickly be decomposed into H_2 and CO [19]. The H_2 profile (*m/e* = 2) presents a desorption initiating at 210 °C, with maximum around 333 °C, that is extended until 480 °C. It is interesting to analyze CO and CO_2 desorption: the *m/e* = 28 profile presents a peak of low intensity, with maximum at 357 °C, and another one around 550 °C. A similar profile is observed for *m/e* = 44 signal (CO_2), where also two peaks are shown: the first one, in the range of 300–450 °C, with maximum at 352 °C; and the second, around 550 °C. According to a previous work [15], using TPD-CO_2, we can attribute this two peaks to CO_2 desorption from the basic sites of the zinc oxide and the $ZnAl_2O_4$ phase, respectively. It was also shown, for the samples with up to 18% of ZnO, that the zinc addition affected the density of acid sites of the alumina surface, mainly the Brönsted acid sites. This favors the surface coverage of Zn^{+2} sites (Lewis acid), weaker than the Al^{+3} sites. According to Tatibouet [13], the CO_2 formation is related either to the water gas shift reaction (CO + H_2O) or to the total CO oxidation, which has the oxygen participation from the zinc oxide structure, as well as, to the decomposition of the formic acid. The formic acid rarely is observed, once it is considered as an intermediate in the formation of methyl formate ($HCOOCH_3$).

Fig. 3 presents the desorption profiles for 20TiA sample. The ion mass fragment signal *m/e* = 29 presents peaks at 135 °C and 210 °C. The first peak is related to the molecular methanol and formaldehyde desorption. The peak at 210 °C is similar to both signals *m/e* = 29 and *m/e* = *45*, suggesting DME desorption that corresponds to 39 and 100% relative intensity, respectively. By analyzing the ion mass fragment signal *m/e* = 28 related to CO desorption, it is observed two peaks: the first one at 390 °C, at the same temperature range of methane desorption (*m/e* = 16), and the second between 490 and 700 °C, attributed to CO_2 fragmentation (11% relative intensity), in accordance with *m/e* = 44 signal. It is worth noting that the CO desorption in this sample is characterized by a higher intensity profile than that obtained for other samples. The H_2 desorption (*m/e* = 2) occurs between 290 and 510 °C, with a maximum at 417 °C.

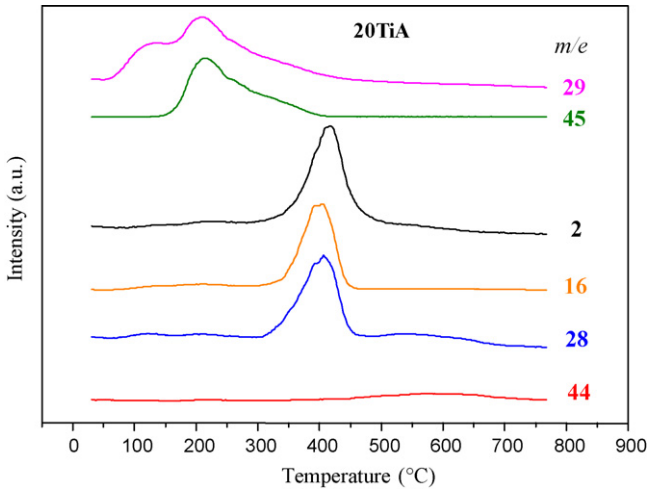

Fig. 3. TPD-MeOH profiles of 20TiA catalyst.

Tatibouet [13], by assuming that a dual acid-base site is needed to adsorb methanol dissociatively on TiO_2, suggests that the formaldehyde would be formed on the less acidic site, which depends on the dehydrogenating ability of the surface, i.e., the O/Ti ratio. The DME formation occurs from the reaction between two adjacent methoxy groups adsorbed on the Lewis acid site of the titanium, a strong (4-fold oxygen coordinated) – and one another mild – (5-fold oxygen coordinated). The dehydrogenating species strongly adsorbed lead to CO desorption and methane would be formed by H transfer to a methoxy group and by the C–O scission.

The integration of the desorption profiles of H_2, CO_2 and CO allowed the quantification (μmol/g) of these species for all the evaluated catalysts and is presented in Table 2. It was observed, for 20TiA, the lowest H_2 and CO_2 formation and the H_2/CO ratio, indicating the basic sites absence and a low dehydrogenating character of the surface. The highest CO production can be attributed to a large density of Lewis acid sites on the TiO_2 surface and to the Lewis and Brönsted acid sites of alumina. These results agree with the literature [20], which demonstrated that the alcohols adsorption at TiO_2 is determined by the local coordination and not by the bulk structure. Besides, are in accordance with surface properties of anatase phase, which the oxygen deficit on the surface favors the alkoxide decomposition and leads to an oxygen deposition on the surface.

The desorption profiles for the catalyst 20ZnTiA are presented in Fig. 4. The desorption profile obtained for the H_2 presents a maximum at 350 °C, whereas the CO_2 desorption has maximum at 357 °C. It is important to observe the shift occurred in the H_2 desorption temperature for the 20ZnA (333 °C) and 20TiA (417 °C) samples. The evaluation of these results suggests an increase in the surface basicity of the 20ZnTiA as compared to 20ZnA, and a loss of the Lewis acid sites density in relation to both, 20TiA and 20ZnA.

Table 2
Quantification of H_2, CO_2 and CO after TPD-MeOH

Sample	H_2 (μmol/g)	CO_2 (μmol/g)	CO (μmol/g)	H_2/CO_2 ratio	H_2/CO ratio
20ZnA	558.8	97.5	28.1	5.7	19.9
20TiA	73.0	0.02	98.1	–	0.7
20ZnTiA	367.9	136.4	31.1	2.7	11.8
20ZnT	148.2	31.3	–	4.7	–

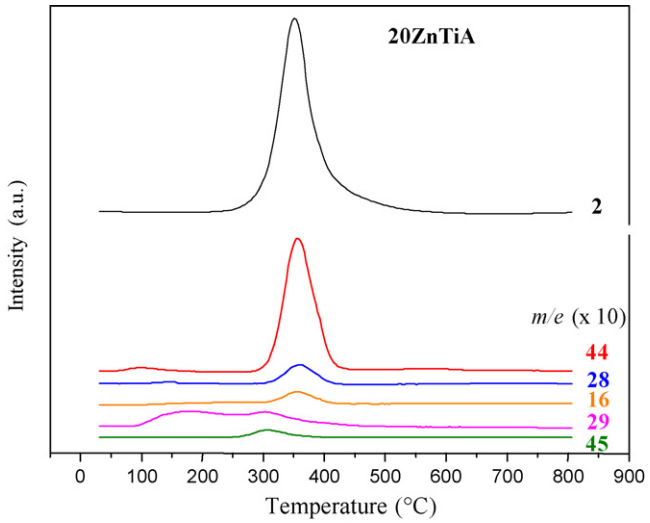

Fig. 4. TPD-MeOH profiles of 20ZnTiA catalyst.

Regarding that zinc loading was constant (20%) for the samples evaluated here and that alumina loading was lower in 20ZnTiA (60%) than in 20ZnA (77%), it evidences that the aluminate formation was lower in the ZnTiA, as showed by XRD results. According to Zou and Shen [12] the formation of this phase is responsible for the Zn^{2+} cations migration into the bulk alumina. It confers a lower basicity to the surface, once increases Al^{+3} sites density on the spinel surface, confirming the highest basic character and the lower density of acid sites on the 20ZnTiA surface with regard to 20ZnA.

As shown in the Table 2, 20ZnTiA and 20ZnA catalysts present greater CO_2 desorption, while 20TiA exhibits the highest CO desorption. These results confirm that the larger density of basic sites and weak Lewis acid sites on the surface can be attributed to zinc oxide, favoring the CO_2 formation. This would also explain the behavior of the catalyst 20ZnT (Fig. 5) that showed only H_2 and CO_2 desorption. This catalyst exhibited an intense H_2 desorption between 250 and 400 °C, with maximum around 310 °C. It is observed for the CO_2 (*m/e* = 44) profile one peak of low intensity, with maximum at around 305 °C. The CO_2 production only, among all the carbon products, characterizes a total decomposition of the alkoxide intermediates, which is related to the following surface properties of this sample:

(i) smallest density of strong Lewis acid sites of titanium oxide;
(ii) presence of basic zinc sites;
(iii) surface oxygen vacancies (characteristic of both oxides, ZnO and TiO_2).

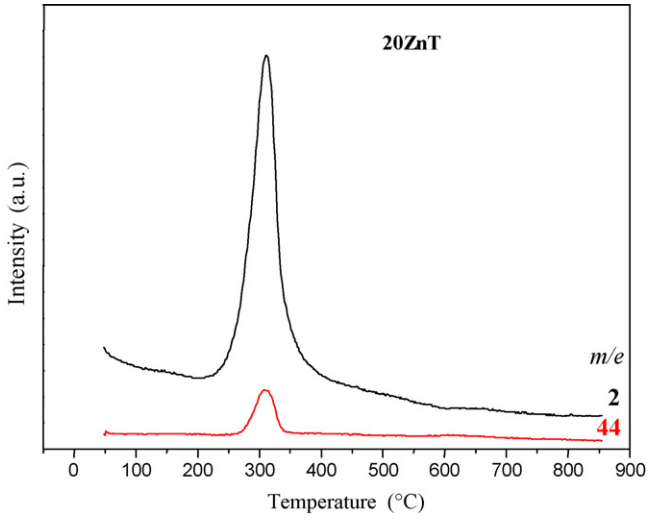

Fig. 5. TPD-MeOH profiles of 20ZnT catalyst.

Therefore, these results have shown that 20ZnT catalyst presented the highest selectivity for H_2 generation from methanol decomposition, considering that methanol was completely decomposed to H_2 and CO_2 and that we do not verified any CO desorption. This points out to the possible application of this catalyst in fuel cells.

4. Conclusions

A series of binary ZnO and TiO_2 oxide catalysts were synthesized maintaining a 20% oxide content on Al_2O_3 support. The same titanium oxide species were found to be present on all catalysts and exhibited high dispersion and a low crystalline structure of anatase phase. The titanium oxide deposition on alumina ($20\%TiO_2/Al_2O_3$) did not cause significant changes of the textural properties of the alumina and favored an undesirable increase in the CO desorption, and therefore, not suitable for use in fuel cells. The impregnation of 20% zinc oxide on the support $20\%TiO_2/Al_2O_3$ confers a redistribution of titanium oxide particles allowing a high interaction of zinc with alumina in the 20ZnTiA catalyst. However, the aluminate phase formation on 20ZnTiA was lower than on 20ZnA catalyst. Thus, the higher Zn^{+2} cations density on 20ZnTiA surface leads an increase in its basicity when compared to 20ZnA. The high H_2/CO_2 ratio obtained for the sample $20\%ZnO/TiO_2$ and the absence of CO desorption in the methanol decomposition is a promising result for its use as support or catalyst to hydrogen production for fuel cells.

References

[1] J.M. Ogden, M.M. Steinbugler, T.G. Kreutz, J. Power Sources 79 (1999) 43.
[2] J. Agrell, H. Birgersson, M. Boutonnet, I. Melián-Cabrera, R.M. Navarro, J.L.G. Fierro, J. Catal. 219 (2003) 389.
[3] L.A. Espinosa, R.M. Lago, M.A. Pena, J.L.G. Fierro, Top. Catal. 22 (3/4) (2003) 245.
[4] B. Lindström, J. Agrell, L.J. Pettersson, Chem. Eng. J. 93 (2003) 91.
[5] M. Manzoli, A. Chiorino, F. Boccuzzi, Appl. Catal. B 57 (2004) 201.
[6] L.F. Brown, Int. J. Hydrogen Energy 26 (2001) 381.
[7] S. Wasmus, A. Kuver, J. Electroanal. Chem. 461 (1999) 14.
[8] D. Chadwick, K. Zheng, Catal. Lett. 20 (1993) 231–242.
[9] T.L. Reitz, S. Ahmed, M. Krumpelt, R. Kumar, H.H. Kung, J. Mol. Catal. A: Chem. 162 (2000) 275.
[10] J. Agrell, H. Birgersson, M. Boutonnet, J. Power Sources 106 (2002) 249.
[11] S.A. El-Hakam, Colloid Surf. A-Physicochem. Eng. Asp. 157 (1999) 157.
[12] H. Zou, J. Shen, Thermochim. Acta 351 (2000) 165.

[13] J.M. Tatibouet, Appl. Catal. A 148 (1997) 213.
[14] L.E. Briand, A.M. Hirt, I.E. Wachs, J. Catal. 202 (2001) 268.
[15] R.A. Vinhas, D.V. Cesar, M. Anacleto, N.S. de Resende, Proc. XIX SiCat, vol. 3, Mérida, September 2004, (2004), p. 4045.
[16] N.S. de Resende, M. Schmal e, J.-G. Eon, J. Catal. 183 (1999) 6.
[17] I.E. Wachs, J.-M. Jehng, W. Ueda, J. Phys. Chem. B 109 (2005) 2275.
[18] L.E. Briand, W.E. Farneth, I.E. Wachs, Catal. Today 62 (2000) 219.
[19] L.A. Espinosa, R.M. Lago, M.A. Peña, J.L.G. Fierro, Top. Catal. 22 (2003) 245.
[20] V.S. Lusvardi, M.A. Barteau, W.E. Farneth, J. Catal. 153 (1995) 41.
[21] A. Yee, S.J. Morrison, H. Idriss, J. Catal. 186 (1999) 279.